Journal of Circuits, Systems, and Computers
Vol. 14, No. 2 (2005) 297–305

A GENERIC MODEL FOR VOLTAGE-CONTROLLED SECOND-ORDER RC SINUSOIDAL OSCILLATORS

A. S. ELWAKIL*

Department of Electrical, Electronic and Computer Engineering,
University of Sharjah, P. O. Box 27272,
Sharjah, United Arab Emirates
elwakil@ee.ucd.ie
elwakil@sharjah.ac.ae

Revised 21 June 2004

A generic model for second-order RC sinusoidal oscillators is derived. The model is based on treating an oscillator as a second-order passive network, with an arbitrary unknown structure, terminated at one port by a linear voltage-controlled negative resistor. A modified model which takes into account the fundamentally nonlinear characteristics of the negative resistor is also derived.

Keywords: Circuit theory; sinusoidal oscillators; nonlinear circuits; voltage-controlled oscillators.

1. Introduction

Sinusoidal oscillators are key elements in a wide variety of electronic systems. Most sinusoidal oscillators are second-order RC active networks with the active element employed as an amplifier, as an integrator or as a general impedance converter. However, it was shown in Refs. 2 and 3 that no matter how the active element is employed, the source of energy in any oscillator circuit can always be localized in a linear negative resistor. Therefore, it should be possible to derive a generic model for all second-order RC sinusoidal oscillators by decomposing the oscillator into a second-order passive network and a linear voltage-controlled negative resistor.

In this work, we derive such a model. We show that no information concerning the particular internal structure of the passive network is needed in order to derive this model. Furthermore, since practical realizations of negative resistors result in fundamentally nonlinear characteristics, we modify the model in order to consider the effect of this nonlinearity. Previously, in Ref. 1, generic models for second-order RC sinusoidal oscillators were derived based on decomposing the oscillator into an

*Permanently with the Egyptian Nuclear Research Center, Cairo, Egypt.

active first-order network of an arbitrary unknown structure, terminated either by a parallel or a series first-order passive RC network.

2. Linear Model

Consider the network shown in Fig. 1 which represents a generic second-order RC active network. The network consists of a second-order passive structure, internally containing two capacitors C_1 and C_2, terminated by a linear voltage-controlled negative resistor r. The voltage across the negative resistor V_r is in general a function of the two state variables of the network, namely the voltages V_{C1} and V_{C2}. Hence, one can write:

$$V_r = q_1 V_{C1} + q_2 V_{C2}\,, \tag{1}$$

where q_1 and q_2 are positive or negative constants.

Any second-order RC network is fully described by the two state equations:

$$I_{C1} = C_1 \dot{V}_{C1} = f_1(V_{C1}, V_{C2}) \quad \text{and} \quad I_{C2} = C_2 \dot{V}_{C2} = f_2(V_{C1}, V_{C2})\,. \tag{2}$$

Since the only source of energy in the network is the negative resistor, one can write:

$$I_r \geq I_{C1} + I_{C2}\,, \tag{3}$$

where $I_r = -V_r/r$ is the current in the negative resistor. We consider here the conservative condition $I_r = I_{C1} + I_{C2}$. Therefore, using Eqs. (1) and (2) in Eq. (3),

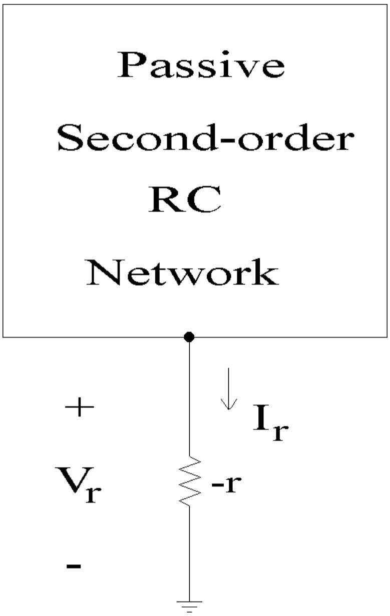

Fig. 1. Generic structure for a voltage-controlled sinusoidal oscillator.

we obtain:

$$-\frac{1}{r}(q_1 V_{C1} + q_2 V_{C2}) = C_1 \dot{V}_{C1} + C_2 \dot{V}_{C2}\,. \tag{4}$$

For simplicity, we assume hereafter that $C_2 = mC_1 = mC$; m is a positive constant. The general state space representation of the network is given by:

$$C\begin{pmatrix} \dot{V}_{C1} \\ m\dot{V}_{C2} \end{pmatrix} = \begin{pmatrix} g_{11} & g_{12} \\ g_{21} & g_{22} \end{pmatrix}\begin{pmatrix} V_{C1} \\ V_{C2} \end{pmatrix}, \tag{5}$$

where $g_{11} \rightarrow g_{22}$ are transconductances. By introducing the following dimensionless variables: $X = V_{C1}/V_{\mathrm{ref}}$, $Y = V_{C2}/V_{\mathrm{ref}}$, $rg_{11} = a_{11}$, $rg_{12} = a_{12}$, $rg_{21} = a_{21}$, $rg_{22} = a_{22}$ and normalizing time with respect to $\tau = rC$, Eq. (5) transforms into:

$$\begin{pmatrix} \dot{X} \\ m\dot{Y} \end{pmatrix} = \begin{pmatrix} a_{11} & a_{12} \\ a_{21} & a_{22} \end{pmatrix}\begin{pmatrix} X \\ Y \end{pmatrix}. \tag{6}$$

Similarly, Eq. (4) transforms into:

$$-(q_1 X + q_2 Y) = \dot{X} + m\dot{Y}\,. \tag{7}$$

For Eq. (6) to possess a pure imaginary eigen pair and hence to admit sinusoidal oscillations, the condition $a_{22} = -ma_{11}$ must be satisfied. In this case, the normalized frequency of oscillation is given by:

$$\omega_n = \sqrt{-\left(a_{11}^2 + \frac{a_{12}a_{21}}{m}\right)}\,;$$

either a_{12} or a_{21} must be negative with the constraint $|a_{12}a_{21}| > ma_{11}^2$. Note that the frequency of oscillation of the sinusoidal oscillator is generally given by: $\omega_0 = \sqrt{n/C_1C_2r^2} = \sqrt{n/m}/Cr$, where n is an arbitrary frequency multiplication constant. Therefore, the normalized frequency of oscillation ω_n is also equal to $\sqrt{n/m}$. One can then rewrite Eq. (6) as:

$$\begin{pmatrix} \dot{X} \\ m\dot{Y} \end{pmatrix} = \begin{pmatrix} a_{11} & a_{12} \\ \frac{-m(a_{11}^2 + \frac{n}{m})}{a_{12}} & -ma_{11} \end{pmatrix}\begin{pmatrix} X \\ Y \end{pmatrix}. \tag{8}$$

It now remains to find a_{11} and a_{12} in order for the network to be fully defined. From Eq. (8), it is seen that:

$$\left[a_{11} - \frac{m(a_{11}^2 + \frac{n}{m})}{a_{12}}\right]X + (a_{12} - ma_{11})Y = \dot{X} + m\dot{Y}\,. \tag{9}$$

Comparing Eq. (9) with Eq. (7) and solving for a_{11} and a_{12}, one obtains:

$$a_{11} = \frac{n + q_1 q_2}{mq_1 - q_2} \quad \text{and} \quad a_{12} = \frac{mn + q_2^2}{mq_1 - q_2}\,. \tag{10}$$

Substituting to Eq. (8) results in:

$$\begin{pmatrix} \dot{X} \\ \dot{Y} \end{pmatrix} = \frac{1}{mq_1 - q_2}\begin{pmatrix} n + q_1q_2 & mn + q_2^2 \\ -\frac{\frac{n}{m}(mq_1 - q_2)^2 + (n + q_1q_2)^2}{mn + q_2^2} & -(n + q_1q_2) \end{pmatrix}\begin{pmatrix} X \\ Y \end{pmatrix}, \tag{11}$$

which represents our target generic model for voltage-controlled sinusoidal oscillators. Recall that on deriving Eq. (11), no information concerning the internal structure of the second-order RC passive network was necessary. In particular, the contribution of the passive network to the model appears via the two voltage transfer constants q_1 and q_2, which will change whenever the network structure changes. The remaining constants, n and m, are arbitrary chosen. We note from Eq. (11) that:

(1) Three expressions dominate the model and appear frequently. These are: $(n + q_1 q_2)$, $(mq_1 - q_2)$ and $(mn + q_2^2)$ with the constraint $mq_1 \neq q_2$.
(2) The special case[a] $m = n = 1$, which results when $C_1 = C_2 = C$ and $\omega_0 = 1/rC$, implies that the model will depend only on the values of q_1 and q_2. If in addition we choose $q_1 = 1$, Eq. (11) simplifies to:

$$\begin{pmatrix} \dot{X} \\ \dot{Y} \end{pmatrix} = \frac{1}{1-q_2} \begin{pmatrix} 1+q_2 & 1+q_2^2 \\ -2 & -(1+q_2) \end{pmatrix} \begin{pmatrix} X \\ Y \end{pmatrix}. \tag{12}$$

Numerical simulations results of Eq. (12) are shown in Fig. 2, which represents the limit cycles observed when setting $q_2 = -1, 0$ and -3, respectively. Note that

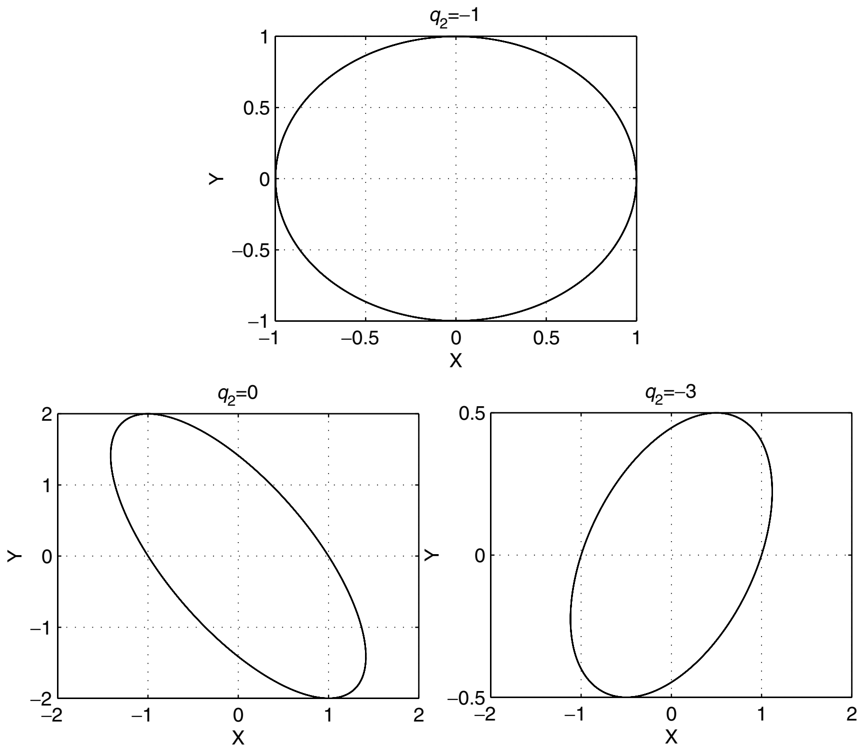

Fig. 2. Limit cycles obtained via numerical simulations of Eq. (12) with $X(0) = 1$ and $Y(0) = 0$. The phase rotation depends on the value of q_2.

[a]This situation is very common and desirable in sinusoidal oscillator design.

$q_2 = -1$ implies that the diagonal of Eq. (12) is all zeros, i.e., it models a quadrature sinusoidal oscillator. This is clear from Fig. 2 where clockwise phase rotation of the limit cycle (X leads Y) can be obtained with $q_2 < -1$ while anti-clockwise phase rotation (X lags Y) can be obtained with $q_2 > -1$. It is worth noting that since Eq. (12) is a linear model, the amplitude of the generated sinusoids is totally dependent on the initial conditions. The initial conditions used to generate Fig. 2 were $X(0) = 1$ and $Y(0) = 0$; changing any of these values automatically results in a limit cycle with different amplitudes. However, it is well-known that practical negative resistors acquire fundamentally nonlinear characteristics which stabilize the amplitude of oscillation independent of the initial conditions. In particular, Eqs. (11) and (12), guarantee the creation of a pure imaginary eigen pair, but in order to start oscillations, this eigen pair needs to be shifted slightly into the right-half complex plane. Without a nonlinear mechanism, which will shift the equilibrium point from the real and unstable origin to another stable but virtual equilibrium point, oscillations will build up unbounded. Therefore, the dynamics of second-order RC sinusoidal oscillators cannot be accurately modeled by Eq. (11). A modified nonlinear model is essential.

3. Nonlinear Model

A popular realization of a voltage-controlled negative resistor is shown in Fig. 3(a) using an op-amp along with its equivalent amplifier-based model. A PSpice simulation of its characteristics for different values of R_1 is shown in Fig. 3(b). It is clear that the resistor current ($I_r = I_i$) is nonlinearly related to the voltage ($V_r = V_i$). The nonlinear characteristics arise from the fact that the amplifier gain K ($K = 1 + R_1/R_2$) is limited by the positive and negative saturation voltages of the op-amp.[3] The N-shaped characteristics of Fig. 3(b) can be modeled as:

$$I_r = I_{BP} \begin{cases} \dfrac{V_0 + V_r}{V_0 - V_{BP}} & V_r < -V_{BP}\,, \\ -\dfrac{V_r}{V_{BP}} & -V_{BP} \le V_r \le V_{BP}\,, \\ \dfrac{V_r - V_0}{V_0 - V_{BP}} & V_r > V_{BP}\,, \end{cases} \tag{13}$$

where $\pm V_0$ are the zero-crossing points of the nonlinear current, $\pm V_{BP}$ are the breakpoint voltages and $\pm I_{BP}$ are the breakpoint currents. Recalling Eqs. (1) and (3), and setting $X = V_{C1}/V_{BP}$, $Y = V_{C2}/V_{BP}$, $V_0/V_{BP} = \Delta$, we obtain:

$$\dot{X} + m\dot{Y} = \begin{cases} \dfrac{\Delta + q_1 X + q_2 Y}{\Delta - 1} & q_1 X + q_2 Y < -1\,, \\ -(q_1 X + q_2 Y) & -1 \le q_1 X + q_2 Y \le 1\,, \\ \dfrac{q_1 X + q_2 Y - \Delta}{\Delta - 1} & q_1 X + q_2 Y > 1\,, \end{cases} \tag{14}$$

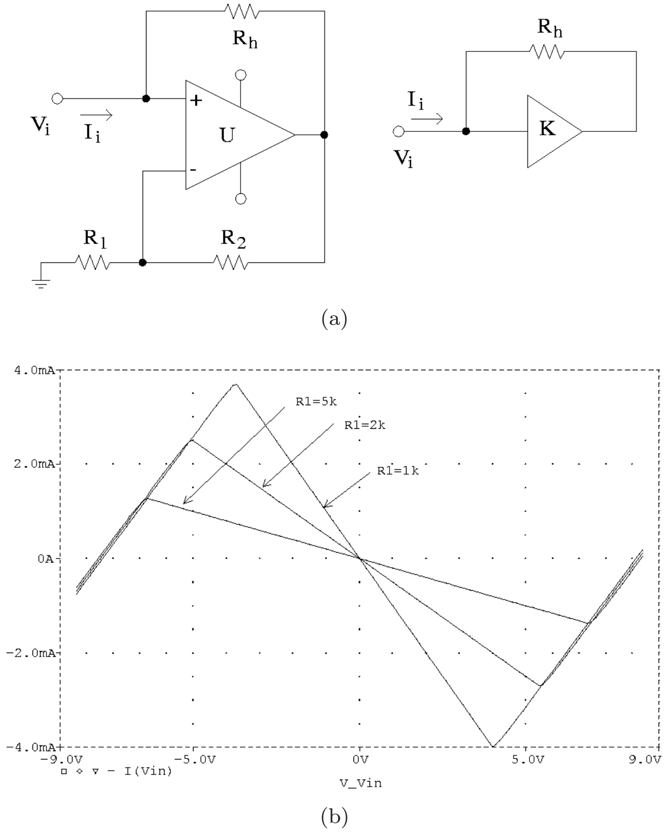

Fig. 3. Realization of a voltage-controlled negative resistor using an op-amp (a) circuit structure and (b) PSpice simulation using an AD712 op-amp biased with $\pm 9\,\text{V}$ supplies, $R_h = R_2 = 1\,\text{k}\Omega$.

which can be written as:

$$\dot{X} + m\dot{Y} = \alpha X + \beta Y + \gamma\,, \tag{15}$$

with

$$(\alpha, \beta, \gamma) = \begin{cases} \left(\dfrac{q_1}{\Delta - 1}, \dfrac{q_2}{\Delta - 1}, \dfrac{\Delta}{\Delta - 1}\right) & q_1X + q_2Y < -1\,, \\ (-q_1, -q_2, 0) & -1 \le q_1X + q_2Y \le 1\,, \\ \left(\dfrac{q_1}{\Delta - 1}, \dfrac{q_2}{\Delta - 1}, \dfrac{-\Delta}{\Delta - 1}\right) & q_1X + q_2Y > 1\,. \end{cases} \tag{16}$$

It is clear that the three-segment piecewise-linear characteristics of Fig. 3(b) imply three equilibrium points, one of which is the origin. Hence, the state space representation of Eq. (8) should be modified to:

$$\begin{pmatrix} \dot{X} \\ m\dot{Y} \end{pmatrix} = \begin{pmatrix} a_{11} & a_{12} \\ \frac{-m(a_{11}^2 + \frac{n}{m})}{a_{12}} & -ma_{11} \end{pmatrix} \begin{pmatrix} X \\ Y \end{pmatrix} + \begin{pmatrix} c_1 \\ c_2 \end{pmatrix}, \tag{17}$$

where c_1 and c_2 are constants. Following a procedure similar to the one followed in the linear model, we obtain:

$$\begin{pmatrix} \dot{X} \\ \dot{Y} \end{pmatrix} = \frac{1}{\beta - m\alpha} \begin{pmatrix} n + \alpha\beta + \epsilon & mn + \beta^2 \\ \frac{\frac{-n}{m}(\beta - m\alpha)^2 - (n+\alpha\beta)^2}{mn+\beta^2} & -n - \alpha\beta \end{pmatrix} \begin{pmatrix} X \\ Y \end{pmatrix} + \begin{pmatrix} c_1 \\ c_1 - \gamma \end{pmatrix}, \quad (18)$$

where α, β and γ are as given by Eq. (16). Note that c_1 is still unknown. For the special case $m = n = 1$, it can be shown that the equilibrium points of Eq. (18) are:

$$x_{\text{eq}} = \frac{(c_1 - \gamma)(1 + \beta^2) + c_1(1 + \alpha\beta)}{\beta - \alpha}, \quad (19a)$$

$$y_{\text{eq}} = -\frac{c_1(\beta - \alpha)^2 + (c_1 - \gamma)(1 + \alpha\beta)(1 + \beta^2) + c_1(1 + \alpha\beta)^2}{(1 + \beta^2)(\beta - \alpha)}. \quad (19b)$$

In the region $-1 \leq q_1X + q_2Y \leq 1$, i.e., for $(\alpha, \beta, \gamma) = (-q_1, -q_2, 0)$, the origin $[x_0, y_0] = [0, 0]$ must be a real equilibrium point. Solving Eq. (19) for c_1 yields $c_1 = 0$. Therefore Eq. (19) simplifies to:

$$[x_{\text{eq}}, y_{\text{eq}}] = \frac{\gamma(1 + \beta^2)}{\alpha - \beta} \left[1, -\frac{1 + \alpha\beta}{1 + \beta^2}\right] \quad (20)$$

with the constraint $\alpha \neq \beta$. Apart from the origin, the other two equilibrium points *must* be virtual,[4] meaning that they lie physically outside the corresponding region of operation ($q_1X + q_2Y < -1$ or $q_1X + q_2Y > 1$) indicated by Eq. (16). This is readily true for all values of $\Delta > 1$ (recall that $\Delta = V_0/V_{BP} > 1$). At these two equilibrium points, it can be shown that the eigenvalues of Eq. (18) are always in the right-half plane and are equal to

$$\frac{\epsilon}{2} \pm j\sqrt{1 + \frac{\epsilon}{q_2 - q_1}\left(\Delta - 1 + \frac{q_1q_2}{\Delta - 1}\right)}.$$

Hence, these two equilibrium points are unstable.

Note that parameter ϵ in Eq. (18) ($\epsilon \to 0$) was added to allow for shifting the imaginary eigen pair around the origin, i.e., in the region $-1 \leq q_1X + q_2Y \leq 1$, slightly into the right-half plane for $\epsilon > 0$. Therefore, at the origin, energy is provided by the negative segment of the nonlinear resistor and oscillations build up. Once the breakpoints are reached, one or the other of the two *virtual and unstable* equilibrium points replaces the origin hence forcing a re-entery to the negative segment of the nonlinear resistor where the unstable origin re-provides energy to the system. This nonlinear mechanism stabilizes the amplitude of oscillation even though the origin is an unstable focus.

Figure 4 represents numerical simulation results, using a fourth-order Runge–Kutta algorithm, of the nonlinear model Eq. (18) with (α, β, γ) as given by Eq. (16) after setting $m = n = q_1 = 1$, $q_2 = -1$ and $\Delta = 2$. The simulations are performed for three values of ϵ; $\epsilon = 0.01$, $\epsilon = 0.05$ and $\epsilon = 0.1$, respectively. The amplitude stabilization is clear from the plotted limit cycles and time waveforms. However, limit-cycle stability is limited to the range $\epsilon < 0.35$ after which trajectories diverge

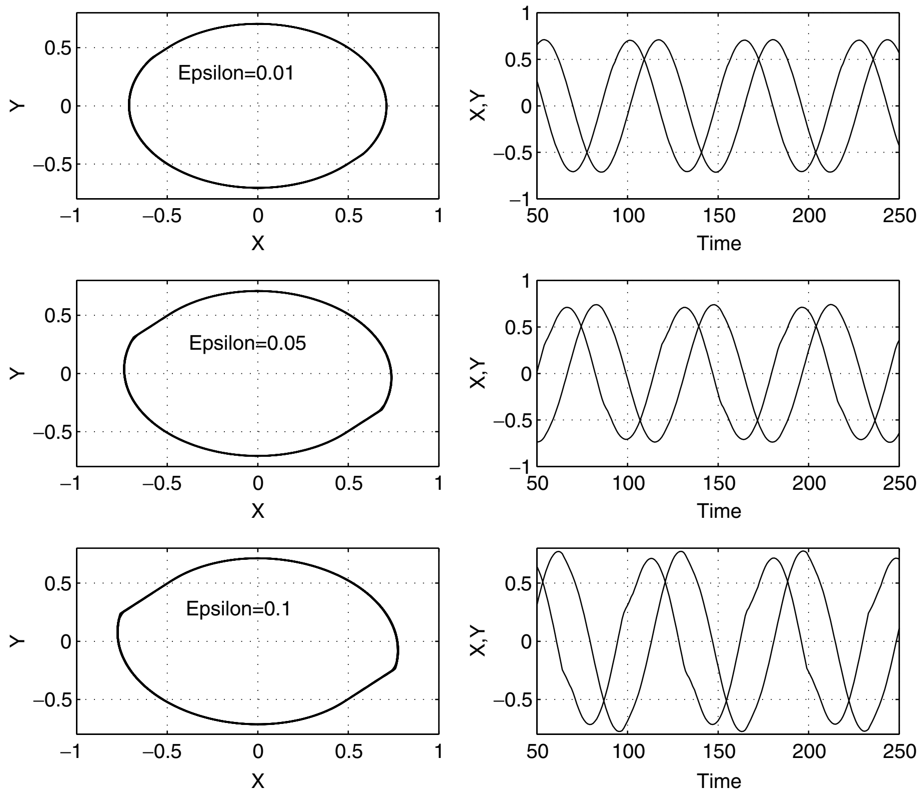

Fig. 4. Numerical simulations of the nonlinear model given by Eqs. (18) and (16) ($m = n = q_1 = 1$, $q_2 = -1, \Delta = 2$).

unbounded and the nonlinearity fails to stabilize the amplitude of oscillation. Distortion in the generated waveforms is also evident as ϵ increases. Note that the equilibrium points corresponding to Fig. 4 are $[0, 0]$ and $2[\pm 1, \mp\epsilon]$.

4. Conclusion

We have derived a generic model for second-order RC sinusoidal oscillators without any information concerning its particular structure but considering only key conditions and assuming energy is localized in a voltage-controlled negative resistor. The model is important in that it highlights the effects of major factors such as the capacitor ratio (m) and the voltage transfer coefficients (q_1, q_2) in general form.

References

1. A. S. Elwakil and M. P. Kennedy, Construction of classes of circuit-independent chaotic oscillators using passive-only nonlinear devices, *IEEE Trans. Circuits Syst. I* **48** (2001) 289–307.

2. S. O. Scanlan, Synthesis of piecewise-linear chaotic oscillators with prescribed eigenvalues, *IEEE Trans. Circuits Syst. I* **48** (2001) 1057–1064.
3. A. S. Elwakil and W. M. Ahmed, On the necessary and sufficient conditions for latch-up in sinusoidal oscillators, *Int. J. Electron.* **89** (2002) 197–206.
4. L. O. Chua, C. A. Desoer and E. S. Kuh, *Linear and Nonlinear Circuits* (McGraw-Hill, 1987).